63. Macrocyclic Tetraethynylethene Molecular Scaffolding: Perethynylated Aromatic Dodecadehydro[18]annulenes, Antiaromatic Octadehydro[12]annulenes, and Expanded Radialenes

by **John Anthony**[a]), **Armen M. Boldi**[a]), **Corinne Boudon**[b]), **Jean-Paul Gisselbrecht**[b]), **Maurice Gross**[b]), **Paul Seiler**[a]), **Carolyn B. Knobler**[c]), and **François Diederich**[a])*

[a]) Laboratorium für Organische Chemie, Eidgenössische Technische Hochschule, ETH-Zentrum, Universitätstrasse 16, CH–8092 Zürich

[b]) Laboratoire d'Electrochimie et de Chimie Physique du Corps Solide, U.R.A. au C.N.R.S. n° 405, Faculté de Chimie, Université Louis Pasteur, 1 et 4, rue Blaise Pascal, B.P. 296, F–67008 Strasbourg Cedex

[c]) Department of Chemistry and Biochemistry, University of California, Los Angeles, California 90024-1569, USA

(29. III. 95)

Tetraethynylethene (3,4-diethynylhex-3-ene-1,5-diyne) molecular scaffolding provided access to novel macrocyclic nanometer-sized C-rich molecules with unusual structural and electronic properties. Starting from *cis*-bis-deprotected *cis*-bis(trialkylsilyl)-protected tetraethynylethenes, the per(silylethynyl)ated octadehydro[12]annulenes **1** and **2** and the corresponding dodecadehydro[18]annulenes **4** and **5** were prepared by oxidative *Hay* coupling. X-Ray crystal-structure analyses of (i-Pr)$_3$Si-protected **2** and Me$_3$Si-protected **4** showed that both annulene perimeters are perfectly planar. Electronic absorption spectral comparisons provided strong evidence that the macro rings in the deep-purple-colored **1** and **2** are antiaromatic ($4n$ π-electrons), whereas those in yellow **4** and **5** are aromatic (($4n + 2$) π-electrons). Although unstable in solution, the antiaromatic compound **2** gave high-melting crystals in which the individual octadehydro[12]annulene chromophores are isolated and stabilized in a matrix-type environment formed by the bulky (i-Pr)$_3$Si groups. Electrochemical studies demonstrated that the antiaromatic octadehydro[12]annulene **2** undergoes two stepwise one-electron reductions more readily than the aromatic chromophore **5**. This redox behavior is best explained by the formation of an aromatic ($4n + 2$) π-electron dianion from **2**, whereas **5** loses its aromaticity upon reduction. The Me$_3$Si derivative **4** was deprotected with borax in MeOH/THF to give the highly unstable hexaethynyl-dodecadehydro[18]annulene **6**, a $C_{30}H_6$ isomer and macrocyclic precursor to a two-dimensional all-C-network. Deprotection of **2** did not give isolable amounts of tetraethynyl-octadehydro[12]annulene **3** due to the extreme instability of the latter. Starting from dimeric and trimeric acyclic tetraethynylethene oligomers, a series of expanded radialenes were obtained. They possess large C-cores with silylethynyl-protected peripheral valences and can be viewed as persilylated C_{40} (**7**), C_{50} (**8**), and C_{60} (**9**) isomers. These expanded C-sheets are high-melting, highly stable, soluble materials which were readily characterized by laser-desorption time-of-flight (LD-TOF) mass spectrometry. Due to inefficient macrocyclic cross-conjugation and/or non-planarity, the extent of π-electron delocalization in **7**–**9** is limited to the longest linearly conjugated π-electron fragment. In agreement with these properties, all three expanded radialenes exhibited similar redox behavior; they are difficult to oxidize but undergo several reversible one-electron reductions in similar potential ranges. Presumably, the reduced π-electron delocalization is also at the origin of the particularly high stability of **7**–**9**.

1. Introduction. – The synthesis of unsaturated all-C and C-rich nanomaterials continues to fascinate chemists. The structural and electronic properties of these compounds are not only of significant theoretical interest, but also promise to lead to new functional materials for use in molecular electronics and optics [1–6]. In the preceding paper, we showed how *acyclic* tetraethynylethene (3,4-diethynylhex-3-ene-1,5-diyne) molecular scaffolding yielded up to 5-nm-long molecular rods with the poly(triacetylene)backbone

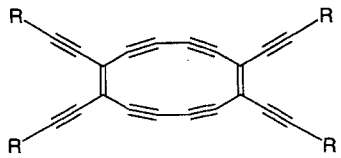

1 R = Me_3Si
2 R = $(i\text{-}Pr)_3Si$
3 R = H

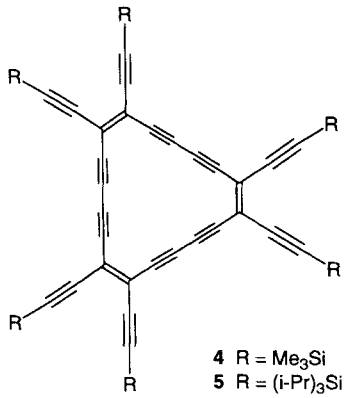

4 R = Me_3Si
5 R = $(i\text{-}Pr)_3Si$
6 R = H

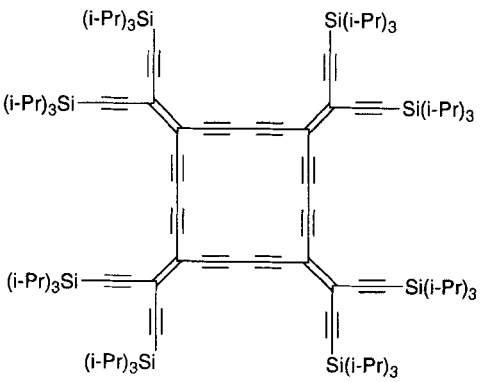

7

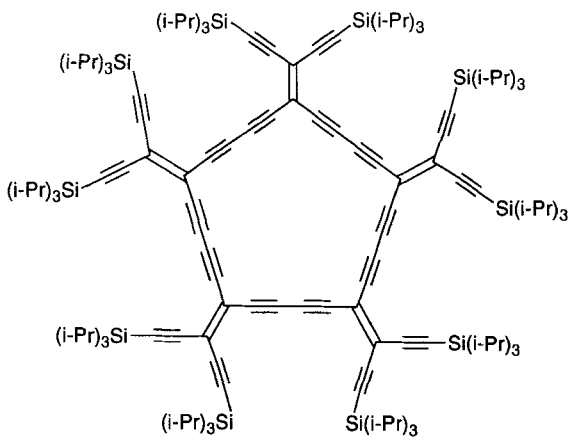

8

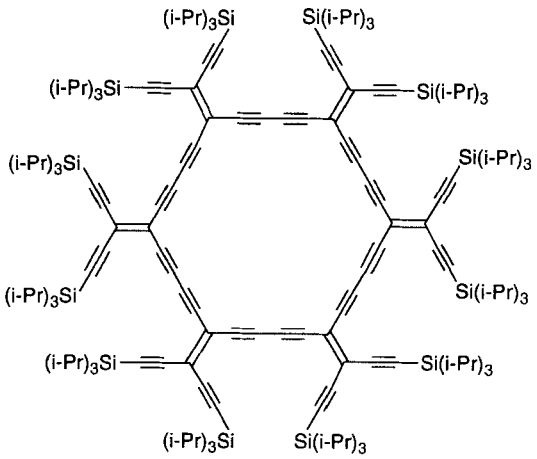

9

[7] as well as cross-conjugated oligomers of the expanded-dendralene type [8]. In this paper, we describe the synthesis and properties of *macrocyclic* tetraethynylethene oligomers including the perethynylated annulenes **1–6** and the expanded radialenes **7–9**. Although dehydroannulenes have been the subject of numerous investigations [9–12], perethynylated derivatives such as **1–6** are unknown. We became interested in their synthesis [13], when we realized that **3** and **6** are macrocyclic precursors to oxidative acetylene polymerizations leading to two-dimensional all-C-networks [2] [14].

Radialenes (see **10**, *Fig. 1*) are a series of all-methylidene-substituted cycloalkanes of molecular formula C_nH_n [15–17] and have attracted much attention for their unusual structural, electronic, and materials properties. Upon insertion of acetylene or diacetylene moieties into the cyclic framework between each pair of vicinal exocyclic methylidene units, the C-rich, previously unknown homologous series of *expanded radialenes* **11** and **12** with the molecular formulae $C_{2n}H_n$ and $C_{3n}H_n$, respectively, are obtained. Compounds **7–9** are the first representatives of the expanded radialenes [18] and can be viewed as persilylated C_{40} (**7**), C_{50} (**8**), and C_{60} (**9**) isomers. Investigations of the properties, in particular stability and solubility, of these extended C-cores were expected to reveal whether even larger persilylated C-sheets, which can be viewed as end-capped C-allotropes [19], are reasonable synthetic targets.

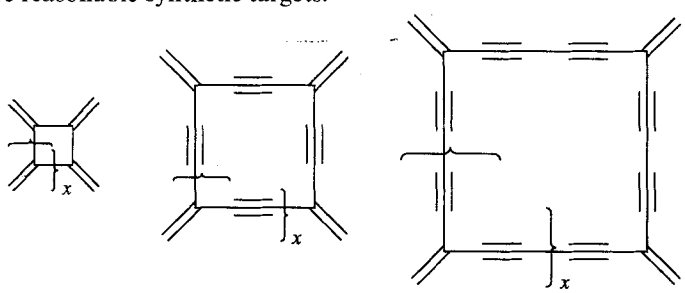

10 C_nH_n **11** $C_{2n}H_n$ **12** $C_{3n}H_n$

Fig. 1. *Progression from radialenes* **10** (C_nH_n) *to the expanded radialenes* **11** ($C_{2n}H_n$) *and* **12** ($C_{3n}H_n$)

2. Results and Discussion. – 2.1. *Syntheses and Structures of Perethynylated Dehydroannulenes. Hay* coupling (CuCl, *N,N,N′,N′*-tetramethylethylenediamine (TMEDA), O_2, acetone) [20] of the *cis*-bis-deprotected tetraethynylethenes **13** and **14** [21] yielded not only the expected dodecadehydro[18]annulenes **4** and **5**, respectively, but also the highly strained octadehydro[12]annulenes **1** and **2**, respectively (*Scheme 1*). Both the total cyclization yield and the ratio of the two formed annulenes varied strongly with concentration (*Table 1*). At low concentrations, the total yield in the reaction of the Me_3Si

Table 1. *Concentration Dependence of the Yields in the* Hay *Cyclization of* **13** *to the Dehydroannulenes* **1** *and* **4**

Concentration [M] of **13**	0.006	0.045	0.08
Product ratio **1**/**4**/higher oligomers[a])	12:5:1	1:4:2	1:3:4
Overall yield [%]	*ca.* 50	*ca.* 45	*ca.* 18

[a]) Acyclic and cyclic higher oligomers.

Scheme 1. *Synthesis of the Perethynylated Dehydroannulenes* **1**, **2**, *and* **4**–**6**

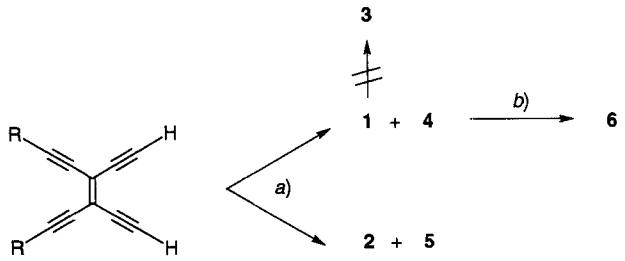

13 R = Me_3Si
14 R = $(i\text{-}Pr)_3Si$

a) CuCl, TMEDA, O_2, acetone, 20°, 1 h; yields in *Table 1*.
b) $Na_2B_4O_7$, MeOH/THF 5:1, 20°, 50 min; quant.

derivative **13** was highest, and dehydro[12]annulene **1** was the dominant product. At higher concentrations, the total yield decreased and **4** became more abundant. In addition, higher cyclic and acyclic oligomers were formed in significant amounts, but could not be isolated in pure form. In the coupling of the $(i\text{-}Pr)_3Si$ derivative **14**, higher cyclic oligomers beyond **5** were not formed, presumably for reasons of steric crowding of the bulky peripheral $(i\text{-}Pr)_3Si$ groups in these macrocycles.

Upon slow recrystallization from pentane solution, the $(i\text{-}Pr)_3Si$-protected octadehydro[12]annulene **2** formed stable, high-melting deep-red crystals suitable for X-ray analysis (*Fig. 2a*). The solid-state structure showed a planar chromophore including the four Si-atoms, with a mean out-of-plane deviation of the conjugated C_{20} framework of 0.089 (6) Å. Considerable strain in the 12-membered ring is expressed by the strong bend in the two butadiyne moieties, with C≡C–C angles as low as 164.5°, and by the reduction of the inner C–C=C bond angles to 117.6 and 118.5° [22] [23]. Comparable C–C=C angles in unstrained tetraethynylethenes adopt values between 120 and 125° [21] [24]. Despite this strain, the molecule is quite stable. At room temperature, dilute pentane solutions remained unchanged over weeks, and crystals were stable to air and light for months. However, if a solution of **2** was concentrated without crystallization, significant decomposition occurred. The high stability of solid **2** clearly derives from the way individual molecules arrange in the crystal.

An examination of the crystal lattice of **2** (*Fig. 2b*) showed that the delicate annulenic cycles are offset in stacking, so that they are completely surrounded by the bulky inert $(i\text{-}Pr)_3Si$ groups. This insulating matrix-type effect of $(i\text{-}Pr)_3Si$ groups has now been observed in several X-ray crystal structures of extended acetylenic compounds and seems to represent a more general mode to stabilize these compounds in the solid state [8] [21].

The Me_3Si derivative **1** is much less stable than **2**, and its deep-purple dilute solutions decomposed slowly by turning brown even when kept in the dark at −20°. In concentrated solutions, **1** decomposed rapidly to a black insoluble material. Deprotection of **1** with sodium tetraborate (borax) in MeOH/THF, which is the mildest method for the deprotection of Me_3Si-substituted alkynes [25], was rapid and quantitative, but decomposition of the formed parent $C_{20}H_4$ chromophore **3** occurred immediately upon evaporation of solvent. Even in dilute solution, **3** decomposed rapidly and could, therefore, not be characterized.

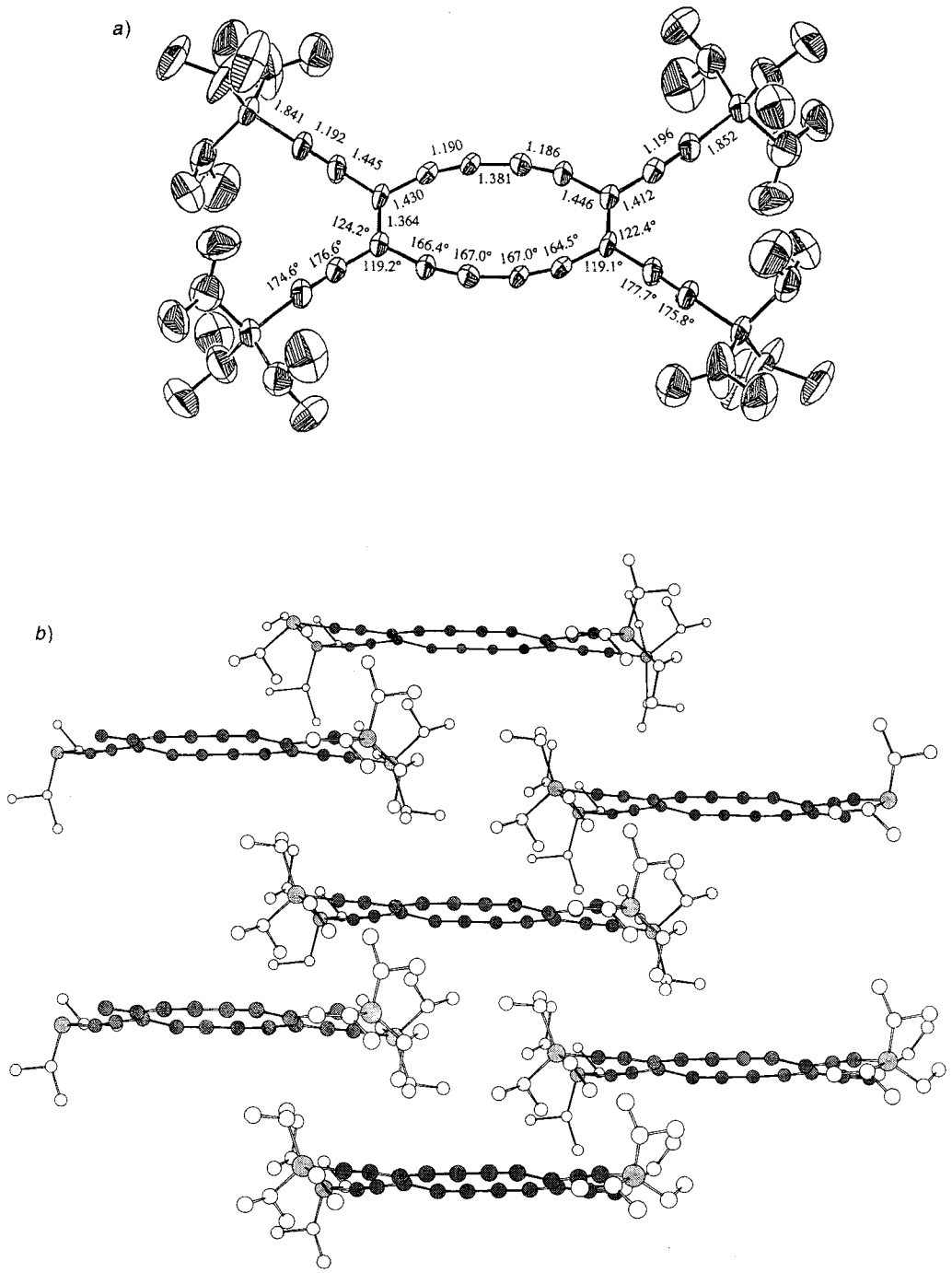

Fig. 2. a) *X-Ray crystal structure of* **2**; b) *crystal lattice of* **2** *showing the conjugated* C_{20} *chromophores* (dark) *fully surrounded by the bulky* $(i\text{-}Pr)_3Si$ *groups*

The protected dodecadehydro[18]annulenes **4** and **5** are both bright-yellow compounds. The $(i\text{-}Pr)_3Si$ derivative **5** formed a stable greasy solid, while Me_3Si-protected **4** gave a crystalline compound which tended to decompose slowly. Solutions of **5** were stable while those of **4** decomposed slowly over time.

Crystals of **4** suitable for X-ray analysis were grown over 9 months by slow evaporation of hexane at −20°. The crystal structure (*Fig. 3*) showed a perfectly planar molecule with the largest out-of-plane deviation within the conjugated C_{30} framework of 0.074 Å. The butadiene moieties in the [18]annulene perimeter are practically linear, and the inner C=C−C bond angles adopt values close to those seen for comparable angles in the X-ray structures of acyclic, strain-free tetraethynylethenes.

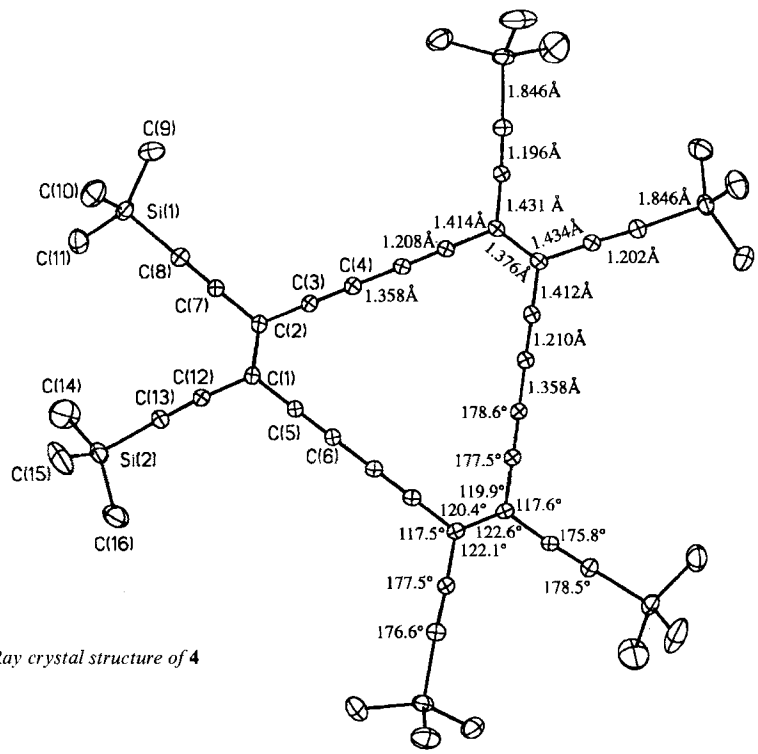

Fig. 3. X-Ray crystal structure of **4**

The [18]annulene **4** could be deprotected with sodium tetraborate (borax), yielding rapidly and quantitatively compound **6** with the molecular formula $C_{30}H_6$, an isomer of hexakis(butadiynyl)benzene, of which persilylated and peralkylated derivatives are known [26]. Other methods described for the deprotection of Me_3Si-substituted alkynes led to instantaneous decomposition for the product. Dilute yellow solutions of **6** are stable for h at room temperature and for a few days at −20° in the dark. Although samples of **6** in $CDCl_3$ concentrated enough for NMR studies decomposed within min, its ^1H- and ^{13}C-NMR spectra could be obtained. The ^1H-NMR spectrum of the decomposed solution showed a series of peaks in the aromatic region, but no single decomposition product could be isolated in pure form. The stability of solutions of **6** is sufficient for use in

oxidative acetylenic coupling reactions, and the preparation of a two-dimensional all-C-network starting from **6** [2] [14] is now under investigation.

2.2. *On the Aromaticity of the Peralkynylated Octadehydro[12]annulenes and Dodecadehydro[18]annulenes.* According to the *Hückel* rule, the planar, cyclic conjugated [12]annulene perimeter in **1** and **2** should be antiaromatic and the [18]annulene perimeter in **4–6** aromatic. However, in the absence of protons in proximity to the chromophores, the expected diatropic character of the $(4n + 2)$ π-electron perimeters and the paratropicity of the $4n$ π-electron systems could not be derived experimentally from common ^{1}H-NMR methods. Therefore, we analyzed in detail the UV/VIS spectra of our compounds in comparison to those of related, known annulenes, to determine whether the aromatic or antiaromatic character would be reflected in their electronic transitions. For the aromatic systems, a large HOMO-LUMO gap leading to an end absorption at higher energy was expected, whereas the antiaromatic chromophores should show an end absorption at lower energy, reflecting a smaller HOMO-LUMO gap [27].

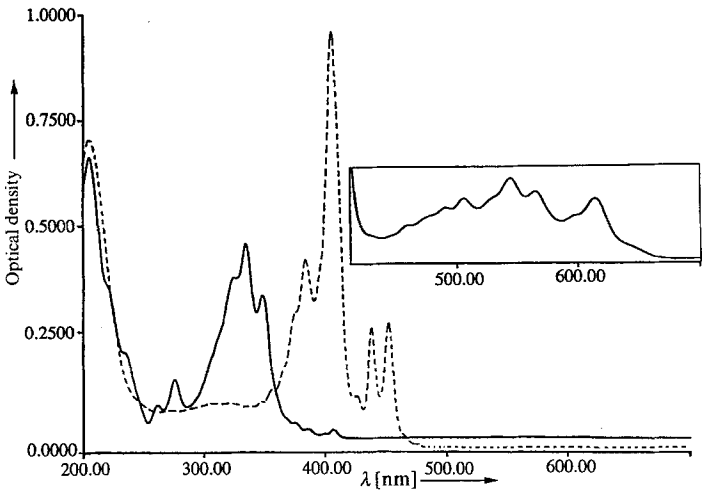

Fig. 4. *Electronic absorption spectra of* **2** (——) *and* **5** (-----) *recorded in pentane. T* 298 K, $d = 1$ cm, $c = 8.0 \cdot 10^{-6}$ M for **5** and $c = 1.02 \cdot 10^{-5}$ M for the shorter- and $2.56 \cdot 10^{-4}$ M for the longer-wavelength absorption (inset) of **2**. Inset is scaled up 25×.

The electronic absorption spectra of $(i\text{-Pr})_3$Si-protected **2** and **5** are shown in *Fig. 4*. Nearly identical spectra were measured for the Me_3Si derivatives **1** and **4**. In agreement with the rigid planar chromophores found in the X-ray crystal structures, the electronic absorption bands of both **2** and **5** show considerable vibrational fine structure. Otherwise the spectra of the two compounds are strikingly different. The end absorption in **5** occurs near 480 nm (2.57 eV), while **2** shows a characteristic weak absorption band at longer wavelength which extends to 660 nm (1.87 eV). In agreement with these spectral data, solutions of **5** are bright-yellow, whereas compound **2** gives purple solutions that, when dilute, look remarkably similar to solutions of buckminsterfullerene in toluene [28].

The large HOMO-LUMO gap of the dodecadehydro[18]annulenes **4** and **5** suggested the assignment of aromatic character to these $(4n + 2)$ π-electron systems. This assign-

ment found strong support in the correlation of the UV/VIS spectra in a series of planar, rigid 1,2,3,4,7,8,9,10,13,14,15,16-dodecadehydro[18]annulenes [24] [29] with macrocyclic perimeters identical to those in **4** and **5**. All these compounds are yellow, and their optical spectra closely resemble, both in terms of band positions and spectral shape, those of **4** and **5** (*Fig. 4*). Their end absorptions appear considerably below 500 nm, which is indicative of a large HOMO-LUMO gap. Their spectra are all characterized by a split longest-wavelength absorption band followed, at lower wavelength, by a very strong band which is structured to higher energy. Since some of these compounds had protons in sufficient proximity to the anulene perimeter, their diatropic character was clearly revealed in the ^{1}H-NMR spectra. We, therefore, conclude that structurally related 1,2,3,4,7,8,9,10,13,14,15,16-dodecadehydro[18]annulenes [30] possess distinct and highly similar electronic absorption spectra with a high-energy end absorption below 500 nm (2.47 eV) and that these spectra can be taken as a strong experimental criterion for the aromatic character of these systems.

The lower-energy end absorption (660 nm, 1.87 eV) and the correspondingly smaller HOMO-LUMO gap of the smaller chromophores **1** and **2** (*Fig. 4*) suggested the assignment of antiaromatic character to these rigid $4n$ π-electron systems. This assignment was also strengthened further in spectral correlations with other dehydro[12]annulenes. With its distinct, structured longest-wavelength band, the spectra of **1** and **2** resemble that of hexadehydro[12]annulene **15**, which has an end absorption at *ca.* 620 nm (1.99 eV) (*Fig. 5*) and is paratropic according to its ^{1}H-NMR spectrum [31]. Some degree of paratropicity was assigned to **16** by using the ^{1}H-NMR criterion, although the conformational flexibility of the cyclohexene rings seems to influence the rigidity of the 12-membered ring as suggested by the reduced vibrational fine structure in the electronic absorption spectrum which extends to *ca.* 550 nm (2.24 eV) [32]. In contrast, **17** [22] [23] and

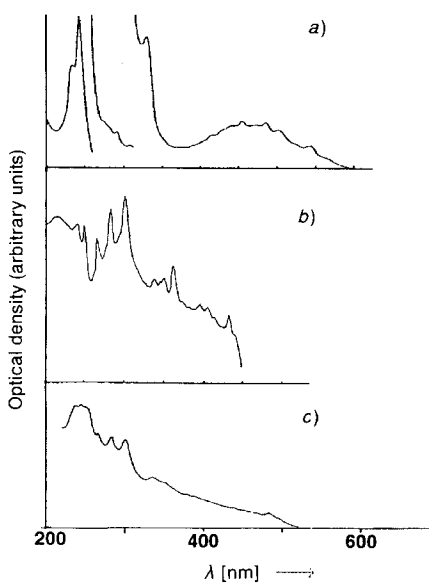

Fig. 5. *Electronic absorption spectra of known [12]annulenes* a) **15** *in isooctane* [31b], b) **17** *in cyclohexane* [32], *and* c) **16** *in* Et_2O [32]

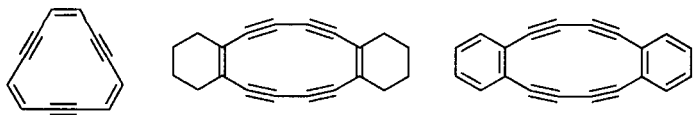

15 **16** **17**

other benz[12]annulenes [33] do not exhibit paramagnetic ring currents as a result of the benzoannelation and show optical properties that differ entirely from those of **1**, **2**, or **15**. Compound **17** is pale yellow, and its end absorption occurs at 450 nm (2.74 eV; *Fig. 5*).

To evaluate the perturbation of the spectra of the dehydroannulenes **1**, **2**, and **4–6** by the presence of the peripheral alkynyl groups, we prepared macrocycles **18** and **19** lacking these groups. The synthesis of these exhaustively (*t*-Bu)Me_2SiOCH_2-substituted annulenes started from diol **20** [21], which was converted into the bis(silyl ether) **21** (*Scheme 2*). Alkynylation to **22**, deprotection to the free *cis*-enediyne **23**, and *Hay* cyclization yielded dark-orange **18** and yellow **19** as stable, crystalline solids. The stability of dehydro[12]annulene **18** in the solid state (dec. at 157°) suggests a protective isolation of the

Scheme 2. *Synthesis of the Dehydroannulenes* **18** *and* **19**

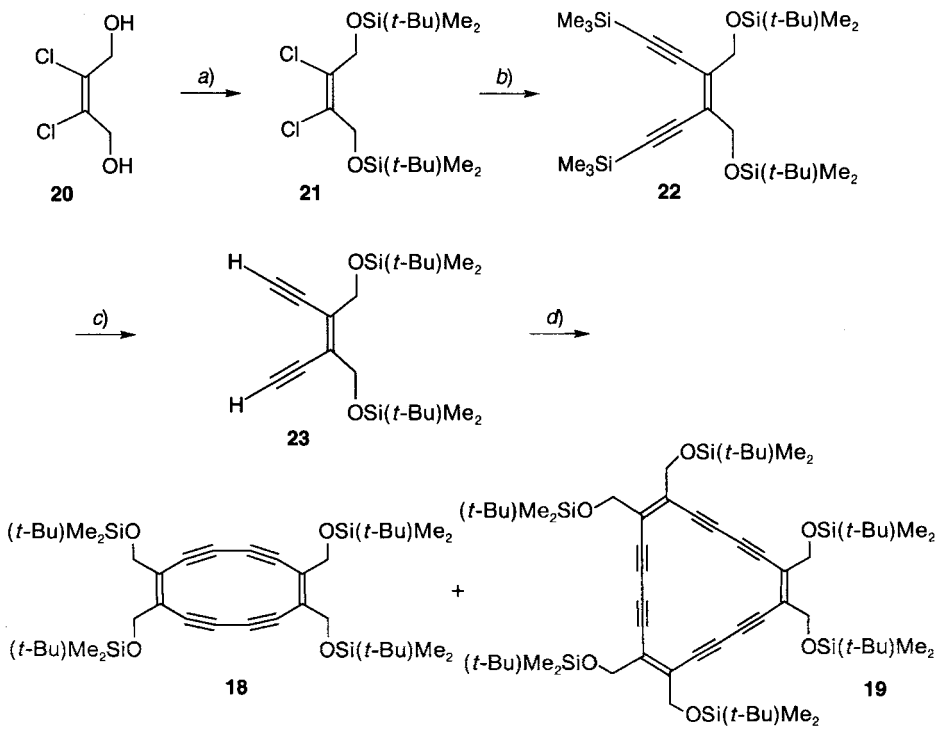

a) (*t*-Bu)Me_2SiCl, 1*H*-imidazole, DMF, r.t., 5 d; 88%. *b*) $Me_3Si{-}C{\equiv}CH$, CuI, $BuNH_2$, $[PdCl_2(PPh_3)_2]$, benzene, r.t., 18 h; 73%. *c*) K_2CO_3, MeOH, r.t., 7 h; 98%. *d*) CuI, TMEDA, acetone, r.t., 12 h; 69% (**18**) and 8% (**19**).

reactive chromophores by the bulky (*t*-Bu)Me_2Si groups similar to that found by X-ray crystallography for **2** (*Fig. 2b*). In solution, **18** was significantly more stable than **2**.

The comparison of the electronic absorption spectra of (*t*-Bu)Me_2SiOCH_2-substituted **18** and **19** (*Fig. 6*) with those of the perethynylated analogs showed that, in each case, perethynylation in **1**, **2**, and **4–6** caused a bathochromic shift of *ca.* 40–50 nm. The greater flexibility of the peripheral groups in **18** and **19** led to a reduction in the vibrational fine structure and to broadened absorption bands as compared to the spectra of the perethynylated derivatives. Otherwise, the comparison showed that the peripheral alkynyl groups in **1**, **2**, and **4–6** did not have a major effect on their UV/VIS absorptions, on which the assignment of aromatic or antiaromatic character was based. In its shape, the spectrum of **19** closely resembles those measured for **4** and **5**, and **19** must also be considered as aromatic. Its end absorption occurs at *ca.* 430 nm (2.88 eV). Similarly to **1** and **2**, octadehydro[12]annulene **18** shows a characteristic long-wavelength band expanding to 620 nm (2.00 eV) and, therefore, can also be considered as antiaromatic.

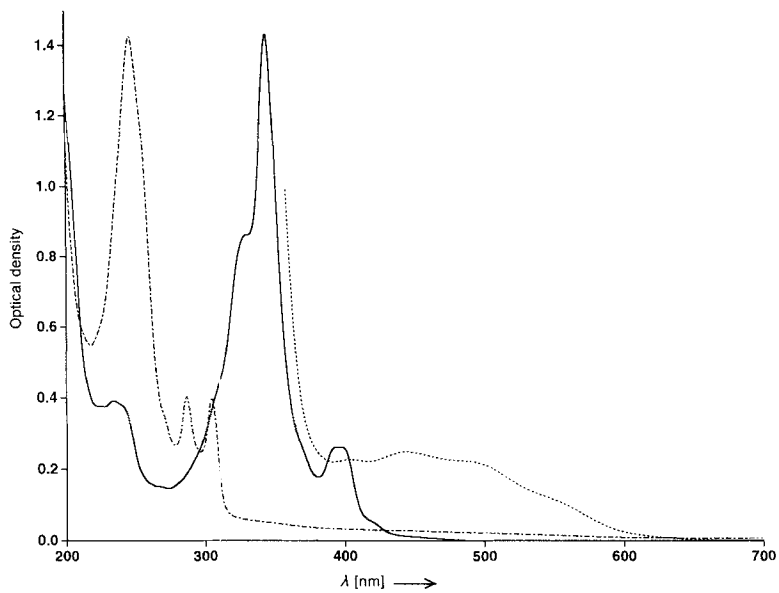

Fig. 6. *Electronic absorption spectra of* **18** ($c = 6.5 \cdot 10^{-5}$ M for the shorter- (–·–·–) and $c = 1.0 \cdot 10^{-3}$ M for the longer-wavelength absorptions (-----)) *and* **19** ($c = 1.59 \cdot 10^{-5}$ M; ——) *in hexane. T* 298 K, *d* = 1 cm.

The presence of protons in close proximity to the annulene perimeters in **18** and **19** allowed us to apply the ^{1}H-NMR criterion for aromaticity, and this provided strong support for the assignments based on the analysis of the electronic absorption spectra. In the ^{1}H-NMR spectrum ($CDCl_3$) of the acyclic reference compounds **22** and **23**, the *s* for the CH_2 protons appeared at 4.29 and 4.34 ppm, respectively. In the paratropic dehydro[12]annulene **18**, the corresponding *s* appeared upfield-shifted at 3.61 ppm, whereas in the diatropic dehydro[18]annulene **19**, the CH_2 protons appeared downfield-shifted at 4.83 ppm.

The aromatic/antiaromatic characteristics of **5** and **2** nicely explain their redox behavior which was analyzed by polarography and cyclic voltammetry (CV) [34]. The dehydro[12]annulene **2** was reduced in two reversible one-electron steps to give a mono- and subsequently a $(4n + 2)$ π-electron dianion (*Table 2*) which were both characterized by spectroelectrochemistry [34]. Due to the loss of aromaticity, the first one-electron reduction of dehydro[18]annulene **5** was more difficult (occurred at more negative potential) than that of **2**. Two additional one-electron reduction steps were observed for **5**. The observed difference in the redox behavior of **2** and **5** was expected based on previous electrochemical studies with $[4n + 2]$ and $[4n]$annulenes [27] [35].

Table 2. *Cyclic Voltammetric Reduction Characteristics of* **2** *on Hg and of* **5** *on a Pt Working Electrode in THF + 0.1* M *$(Bu_4N)PF_6$* [34]

	$E_1'^{\circ a)}$	$E_2'^{\circ a)}$	$E_3'^{\circ a)}$
2	–0.99	–1.46	–
5	–1.12	–1.52	–1.91

a) V *vs.* ferrocene, formal reduction potential $E'^{\circ} = (E_{p_a} + E_{p_c})/2$.

2.3. *Synthesis and Properties of Persilylethynylated Expanded Radialenes.* Initial attempts to prepare the targeted expanded radialenes by oxidative cyclization of geminally bis-deprotected **24** [21] under either *Hay* [20] or *Eglinton-Glaser* [22a] [36] coupling conditions failed (*Scheme 3*). *Cadiot-Chodkiewicz* hetero-coupling cyclizations [37] between **24** and **25** [21] were equally unsuccessful. To favor macrocyclization over competing polymerization reactions, the dimeric tetraethynylethene derivative **26** [8] was used as

Scheme 3. *Unsuccessful Approaches to the Expanded Radialenes* **7–9**

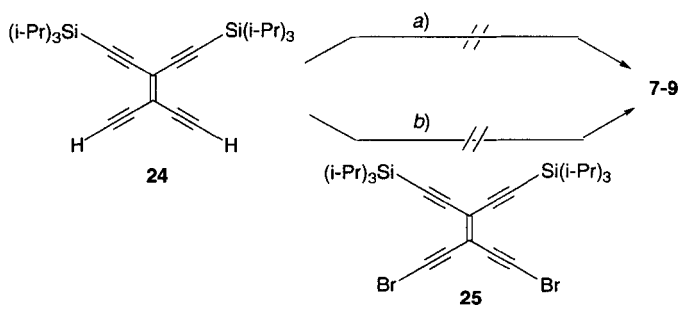

a) Anh. $Cu(OAc)_2$, pyridine, or CuI, TMEDA, O_2, acetone. *b*) CuCl, $NH_2OH \cdot HCl$, $BuNH_2$, DMF/benzene.

the cyclization component and, under *Eglinton-Glaser* conditions, the expanded radialenes **7** and **9** formed in addition to higher, less well characterized oligomers (*Scheme 4*). Oxidative cyclization of dimeric tetraethynylethene **26** with the unstable trimeric **28**, freshly prepared by deprotection of **27** [8], afforded the expanded radialene **8** in addition to small traces of **7** and **9**.

Scheme 4. *Syntheses of the Expanded Radialenes* **7–9**

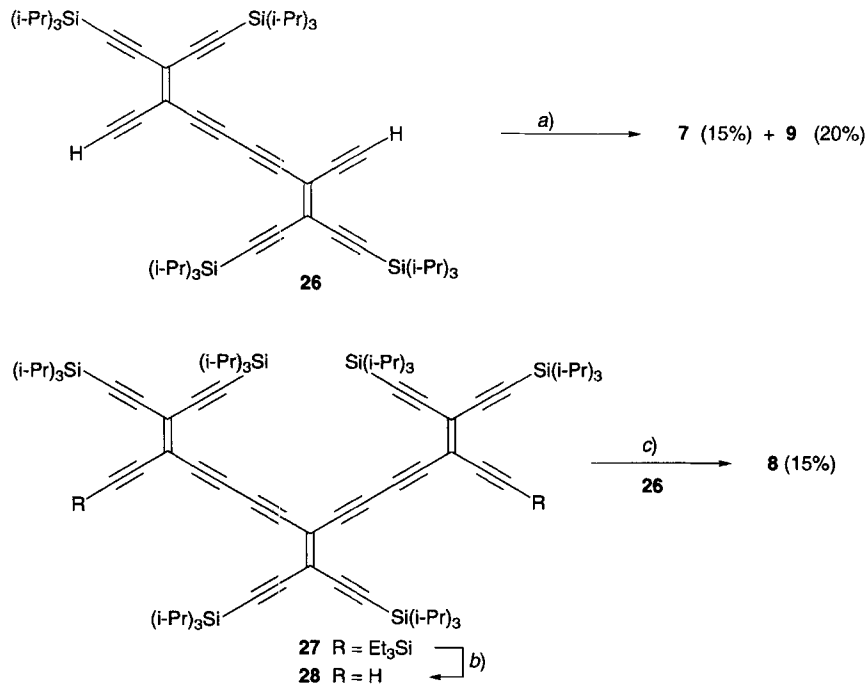

a) Anh. $Cu(OAc)_2$, pyridine/benzene 3:1, r.t., 20 h. *b*) K_2CO_3, MeOH/THF 1:1, r.t., 1 h. *c*) Anh. $Cu(OAc)_2$, pyridine/benzene 3:2, r.t., 20 h.

The end-capped, nanometer-sized C-sheets **7–9** with diameters, not including the $(i\text{-Pr})_3Si$ groups, of *ca.* 17 (**7**), *ca.* 19 (**8**), and *ca.* 22 Å (**9**) are amazingly stable compounds with melting points above 220°. This remarkable stability at ambient atmosphere indicates the absence of free terminal alkyne groups that generally destabilize polyalkyne chromophores [8] [21]. They are readily soluble in all common aprotic solvents. The proposed cyclic structures are supported by the absence of terminal acetylenic signals in the ^{1}H-NMR spectra. Similarly, the IR spectra do not show any ≡C–H stretches; only weak C≡C stretches at 2125 (**7**), 2121 (**8**), and 2124 (**9**) are visible. No C=C stretching bands are observed which is in agreement with the IR spectra of other weakly polar tetraethynylethene derivatives [8] [21]. The ^{13}C-NMR spectra of **7–9** are very similar, and each displays four acetylenic and two olefinic C-resonances, as expected for averaged D_{4h}, D_{5h}, and D_{6h} molecular symmetries, respectively. The sp^2-C-atoms resonate between 114 and 122 ppm, the sp-C-atoms of the central butadiyne moieties between 82 and 86 ppm, and the sp-C-atoms of the peripheral $(i\text{-Pr})_3Si$–C≡C groups between 103 and 107 ppm.

As in previous studies with large C-rich materials [6] [8] [17] [38], laser-desorption time-of-flight (LD-TOF) mass spectrometry [39] was a powerful method in the characterization of the expanded radialenes. The molecular weight of the three macrocycles was confirmed in the spectra recorded in the linear mode with negative-ion detection. Positive ions of **7–9** could not be detected. The spectra exhibited strong molecular ions in the

expected m/z range as well as a complete absence of any fragmentation or impurity peaks [18]. The formation and detection of anions in the gas phase suggested that the expanded radialenes, similar to other conjugated C-rich materials [7] [8] [34], can be electrochemically reduced, and this hypothesis induced the studies of their redox behavior described below.

Due to steric interactions between the bulky peripheral $(i\text{-Pr})_3Si$ groups, distortions of the geometries of **7–9** from planarity are expected, particularly in the larger macrocycles. In the absence of X-ray crystallographic data, the extent of these distortions remains uncertain. AM1 Calculations indicate that all three expanded radialenes distort significantly out of planarity. However, the pronounced vibrational fine structure of their electronic absorption spectra (*Fig. 7*) also suggests that the macrocycles have strong conformational preferences and are not very flexible [24] [40].

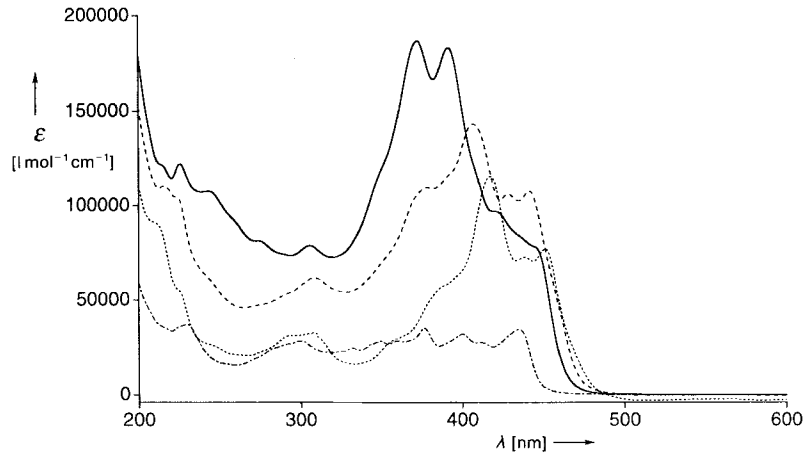

Fig. 7. *Electronic absorption spectra of* **29** (– · – · –), **7** (· · · · ·), **8** (-----), *and* **9** (——) *in hexane. T* 298 K.

Despite their high degree of unsaturation, **7–9** are yellow colored, indicating the existence of only a weak macrocyclic π-electron conjugation. This assumption is clearly supported by a comparison between the UV/VIS spectra of **7–9** and **29** [8]. Compound **29** contains the 3,4,9,10-tetraalkynyl-substituted dodeca-3,9-diene-1,5,7,11-tetrayne chromophore in a preferred '*transoid*' array with respect to the central butadiyne moiety; in the enforced '*cisoid*' array, this is also the longest linearly-conjugated π-electron fragment in the macrocycles. The spectral end absorption changes little between **29** and **7–9** and, within the macrocyclic series, it even remains almost constant. This is similar to the situation previously encountered for the expanded dendralenes such as **31** [8]. π-Electron delocalization in **7–9** extends efficiently only through the longest linearly conjugated fragment, and the measured linear increase in the extinction coefficient of the strongest absorption band with increasing ring size presumably results from the increasing number of such fragments in the macrocycles. It is at present uncertain, whether the strongly reduced extent of π-electron delocalization in **7–9** is mainly due to inefficient macrocyclic cross-conjugation – an explanation which we tend to favor – or the non-planarity of the rings.

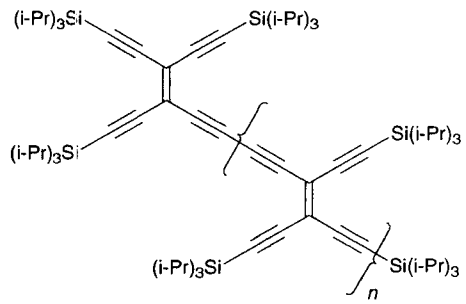

29 $n = 1$
30 $n = 2$

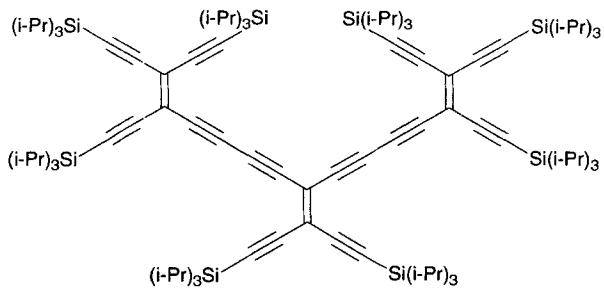

31

2.4. *Electrochemical Properties of the Expanded Radialenes.* The redox properties of the expanded radialenes, in comparison to those of **29–31** [8] [34] were examined by polarography and cyclic voltammetry (CV) in THF with $(Bu_4N)PF_6$ (0.1M) as the supporting electrolyte. The working electrode was either Pt or Hg, and the reference electrode Ag/AgCl. The results of the CV measurements are given in *Table 3*; they are in very good agreement with the data obtained in the polarographic studies. All redox potentials shown are referred to the ferrocene/ferrocenium (Fc/Fc^+) redox couple.

Both transient (CV) and stationary (polarography) redox methods showed that the expanded radialenes **7–9** underwent several distinct reduction steps. No oxidation occurred at potentials below 1.0 V (*vs.* Fc/Fc^+). The first reduction potentials did not

Table 3. *Cyclic Voltammetric Reduction Characteristics of the Expanded Radialenes* **7–9** *in Comparison to* **29–31** *on a Hg* (**29, 30**) *or a Pt* (**7–9, 31**) *Working Electrode in THF + 0.1M* $(Bu_4N)PF_6$

	E'^{o}_1[a])	E'^{o}_2[a])	E'^{o}_3[a])	E'^{o}_4[a])
29[b])	–1.52	–1.89	–2.90[c])	
30[b])	–1.23	–1.47[c])	–	
31[b])	–1.36	–1.74	–	
7	–1.08	–1.28	–	
8	–1.35	–1.64	–1.94[c])	
9	–1.27	–1.67	–1.81	–1.98

[a]) V *vs.* ferrocene, formal reduction potential $E'^{o} = (E_{p_a} + E_{p_c})/2$. [b]) See [34]. [c]) Peak potential E_{p_c} for irreversible reduction.

dramatically differ from those measured for the acyclic comparison compounds **30** and **31**. This is strong indication that the extent of π-electron conjugation in the macrocycles is not significantly larger than in the smaller acyclic derivatives with reduced chromophores. The greater ease of reduction of the smallest derivative **7**, compared to **8** and **9**, could indicate that this compound is more planar as a result of less steric interactions between the peripheral $(i\text{-Pr})_3Si$ goups. Whereas the two reductions for **29–31** and **7** and **8** correspond with a very high probability to one-electron steps, this is not clearly ascertained for the 2nd to 4th reduction steps of **9**. The latter reduction steps exhibited smaller reduction currents than the first one, and it cannot be entirely excluded, based on the present data, that they might correspond to the reduction of chemical species produced by a chemical transformation of the radical anion generated after the first reductive electron transfer.

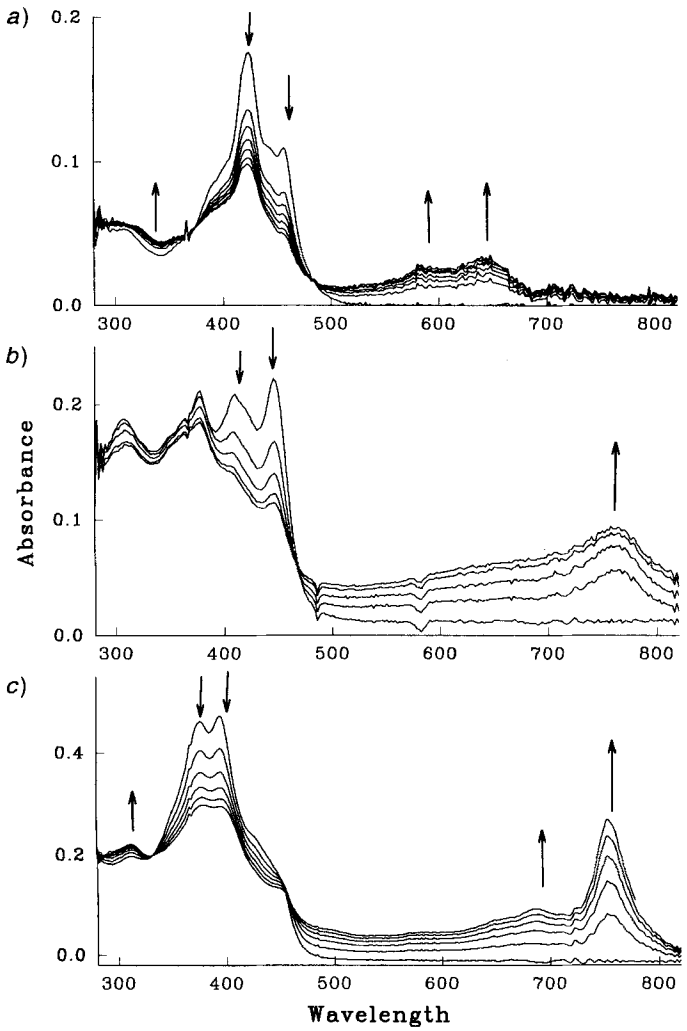

Fig. 8. *UV/VIS Spectra recorded every 10 s during microelectrolysis on a Pt optically transparent thin-layer electrode* (OTTLE) *in* $CH_2Cl_2 + 0.1$ M $(Bu_4N)PF_6$ *for the first reduction step of* a) **7** (applied potential of −1.15 V *vs.* Fc/Fc^+), b) **8** (applied potential of −1.40 V *vs.* Fc/Fc^+), *and* c) **9** (applied potential of −1.30 V *vs.* Fc/Fc^+)

Microelectrolytic reductions were also performed in thin-layer cells, to obtain the electronic absorption spectra of the reduced species and to ascertain whether, on the time scale of the microelectrolysis (typically 60–120 s), the reduced species are stable or not and, therefore, to check whether the reduction may be reverted to regenerate the initial species.

Upon transfer of the first electron, the intensity of the long-wavelength bands (above 320 nm, *Fig. 8*) of all three expanded radialenes decreased, while the weak band at *ca.* 310 nm decreased in the spectrum of **8** but increased slightly in that of **7** and **9**. Simultaneously, new bands emerged at longer wavelength: **7** gave new bands at 590 and 640 nm, **8** at 760 nm, and **9** at 685 and 760 nm. The first reduction step could be totally reverted on the microelectrolytic time scale, restoring the initial spectrum and, therefore, the unchanged neutral expanded radialene. The presence of isosbestic points in thin-layer spectroelectrochemical measurements (*Fig. 8*) is expected for two species in equilibrium, namely the neutral initial species and the generated radical anion of **7**–**9**.

Upon the second reduction step, **7** showed new absorption bands at 700 and 780 nm, whereas all the shorter-wavelength absorptions decreased in intensity. On the contrary, no new absorption bands were observed after the second reduction of **8** and **9** within the cut-off wavelength (820 nm) of the UV/VIS spectrometer. Therefore, if new bands resulted from the second reduction of **8** and **9**, they would be located beyond 820 nm. Microelectrolysis as well as cyclic voltammetric spectroelectrochemistry at rather low scan rate (20 mV/s) indicated that the species resulting from the second reduction of **7**–**9** were not stable, even not for a few seconds, and underwent irreversible chemical reactions. Following the second reduction, restoration by reoxidation of the initial expanded radialene species and of the corresponding absorption spectrum was not possible. When the scan rate of the spectroelectrochemical CV measurement was raised from 20 to 100 mV/s, the backward scan restored in part the initial spectrum, as was shown for **9**. This behavior could be expected from the shorter time window allowed for the chemical reaction of the dianion to occur at the higher scan rate.

3. Conclusions. – With the perethynylated dehydroannulenes **1**, **2**, **4**, and **5** and the expanded radialenes **7**–**9**, nanometer-sized C-sheets incorporating up to 24 C≡C bonds (**9**) were prepared. With their peripheral end-capping silyl groups, these flat compounds are remarkably soluble and, therefore, fully characterizable. They are difficult to oxidize – no oxidation wave below 1.0 V *vs.* Fc/Fc^+ was observed in their cyclic voltammograms – and undergo multiple one-electron reduction steps. Similar redox behavior was observed for large molecular C-rods and polymers with the all-C poly(triacetylene) backbone [8] [41] and seems to represent a characteristic property of unsaturated acetylenic C-rich molecules and presumably also C-allotropes. Since the fullerenes C_{60} and C_{70} as well as many of their adducts exhibit similar properties [42], such redox behavior may be a general phenomenon for unsaturated forms of C.

Whereas the perethynylated annulenes are quite reactive, including the *Hückel*-aromatic 18π-electron systems, the perethynylated expanded radialenes are amazingly stable molecules. Differences in the extent of the macrocyclic π-electron delocalization account for this observation. The annulenes are destabilized since the macrocyclic perimeters are fully linearly conjugated. In the expanded radialenes, cross-conjugation, and possibly non-planarity, drastically reduce the extent of π-electron delocalization, and, thereby,

stabilize the molecules. The electronic absorption spectra of **7–9** suggest that cross-conjugation cannot compete with linear conjugation and that π-electron delocalization is limited to the longest linearly conjugated fragment in these systems. A reduced π-electron conjugation in **7–9** is also apparent from the redox behavior of these compounds. As previously noted [2] [8], the limitation of π-electron delocalization due to inefficient cross-conjugation may be a general stabilizing principle of unsaturated C-based matter. This principle may serve as a useful and previously unrecognized guideline in the synthetic targeting of large all-C-molecules and networks. The high solubility and high stability of the expanded radialenes raises great hope that much larger C-surfaces can be prepared and handled as long as the peripheral valences contain stabilizing and solubilizing groups such as the $(i\text{-Pr})_3Si$ groups in **7–9**. A further expansion of the molecular dimensions will yield compounds which resemble large graphite or diamond fragments in that the C-surfaces (rather than the heterofunctions at the peripheral valences) determine their materials properties.

In the absence of ^{1}H-NMR spectral information due to the lack of H-atoms, the analysis of the electronic and structural properties of all-C-perimeters relies heavily upon the optical spectra of these materials. This was nicely illustrated by the present study. UV/VIS Spectral correlations allowed the assignment of aromatic character to the dodecadehydro[18]annulenes **4** and **5** and antiaromatic character to the octadehydro-[12]annulenes **1** and **2**. Also, the reduced π-electron delocalization in the expanded radialenes was revealed in the electronic absorption spectra. Another extremely useful technique in the analysis of C-rich and all-C materials is laser-desorption time-of-flight (LD-TOF) mass spectrometry with and without matrix assistance. The search for novel C-materials with unusual properties not only brings synthetic chemistry closer to the fertile interface with materials science [2] but also enriches the chemical efforts by the need for incorporation of the latest advances in analytical techniques.

This work was supported at *UCLA* by the *U.S. National Science Foundation* and the *Office of Naval Research* and at ETHZ by a grant from the *Swiss National Science Foundation* and ETH setup funds. *J. A.* was supported at UCLA by a graduate-student fellowship from the *American Chemical Society*. We thank Dr. *W. Amrein* for help with the LD-TOF mass spectra.

Experimental Part

General. See [8] [21].

Laser-Desorption Time-of-Flight Mass Spectrometry (LD-TOF): See [8].

X-Ray Crystal Structure of **4**. Crystal data at 265 K for $C_{48}H_{54}Si_6 \cdot C_6H_{14}$, ($M_r$ 885.7): rhombohedral (hex. setting), space group $R\bar{3}$ (No.148), $\rho_{calc.} = 1.00\ g\,cm^{-3}$, $Z = 6$, $a = b = 25.145(6)$, $c = 16.065(4)$ Å, $V = 8796(4)$ Å^3. *Enraf-Nonius-CAD4* diffractometer, CuK_α radiation, λ 1.5418 Å. Single crystals (*ca.* 0.3 × 0.3 × 0.3 mm) were obtained by slow evaporation (9 months at –20°) of a hexane soln. The structure was solved by direct methods and refined by full-matrix least-squares analysis (SHELXTL PLUS), using an isotropic extinction correction and an exponentially modified weight factor $r = 5$ Å^2. Final $R(F) = 0.057$, $wR(F) = 0.063$ for 209 variables and 2508 observed reflections with $I > 3.0\ \sigma(I)$ and $\theta < 65°$ (heavy atoms, anisotropic; H-atoms, isotropic; H-positions based on stereochemical considerations). The molecular geometry is given in *Fig. 3*. Further details of the crystal-structure investigations are available on request from the *Cambridge Crystallographic Data Centre*, 12 Union Road, Cambridge CB2 1 EZ (UK), on quoting the full journal citation.

1,2,7,8-Tetrakis[(trimethylsilyl)ethynyl]-3,4,5,6,9,10,11,12-octadehydro[12]annulene (**1**) *and 1,2,7,8,13,14-hexakis[(trimethylsilyl)ethynyl]-3,4,5,6,9,10,11,12,15,16,17,18-dodecadehydro[18]annulene* (**4**). To a soln. of **13**

[21] (0.24 g, 0.9 mmol) in acetone (150 ml) open to the air was added *Hay* catalyst (1 ml, *ca.* 0.2 mmol of a soln. prepared by stirring CuCl (2.5 g, 25 mmol) and TMEDA (1.25 ml, 0.96 g, 9 mmol) in acetone (45 ml) for 30 min). After stirring for 1 h, the black soln. was poured into pentane and extracted with H_2O and then sat. aq. NaCl soln. Filtration through a short plug (SiO_2, pentane) yielded a deep-purple fraction of **1**, and subsequent elution with hexane/CH_2Cl_2 1:1 gave a bright-yellow fraction. The purple fraction containing pure, highly unstable **1** (79 mg, 33%) was rapidly evaporated and analyzed. Evaporation to *ca.* 5 ml and standing overnight at −20° gave a dark brown soln. Eventually, a black solid, indicative of complete decomposition was obtained. **1**: UV/VIS (pentane): 220 (sh), 233 (sh), 262, 276, 327, 336, 349, 374, 385, 402 (sh), 408, 462, 477 (sh), 493, 506, 545, 566, 600 (sh), 612; no ε's since the instability of **1** did not allow to weight in with any accuracy. IR (KBr): 2144 (C≡C). ^{1}H-NMR (500 MHz): 0.162 (*s*, 36 H). ^{13}C-NMR (125.8 MHz): −0.45; 88.99; 93.67; 97.53; 109.6; 125.5. DEI-MS (20 eV): 532 ($M^{+\cdot}$).

The yellow fraction was evaporation: **4** (33 mg, 14%). Greasy crystalline solid. M.p. 195° (dec.). UV/VIS (pentane): 204 (88700), 248 (sh, 14900), 303 (11000), 356 (sh, 18300), 374 (sh, 43800), 383 (59000), 403 (125700), 425 (sh, 15800), 437 (35200), 452 (35600). IR (KBr): 2122 (C≡C). ^{1}H-NMR (500 MHz): 0.323 (*s*, 54 H). ^{13}C-NMR (125.8 MHz): −0.30; 84.21; 84.84; 99.88; 110.0; 118.9. MALDI-TOF-MS 799 (M^+). X-Ray: *Fig. 3*.

Higher acyclic and cyclic oligomers were only eluted as mixed fractions and could not be isolated or purified.

1,2,7,8-Tetrakis[(triisopropylsilyl)ethynyl]-3,4,5,6,9,10,11,12-octadehydro[12]annulene (**2**) *and 1,2,7,8,13,14-hexakis[(triisopropylsilyl)ethynyl]-3,4,5,6,9,10,11,12,15,16,17,18-dodecadehydro[18]annulene* (**5**). To a soln. of **14** [21] (0.89 g, 0.002 mol) in acetone (500 ml) open to the air was added *Hay* catalyst (1 ml, *ca.* 0.2 mmol; prepared as described in the synthesis of **1** and **4**). After stirring for 1 h, the black mixture was poured into pentane and extracted with 0.1N HCl, then H_2O, and sat. aq. NaCl soln. Filtration through a short plug (SiO_2, hexane) afforded a deep-purple fraction of **2** followed by the bright-yellow fraction of **5**. The purple fraction was evaporated to 10 ml and then stored at −20° overnight to yield **2** (0.24 g, 27%). M.p. 200° (dec.). Deep-red needles, suitable for X-ray analysis. UV/VIS (pentane): 220 (sh, 35200), 233 (sh, 19600), 262 (7200), 276 (13200), 325 (36900), 335 (44700), 349 (32600), 374 (sh, 3110), 385 (sh, 1690), 402 (sh, 570), 407 (1540), 461 (200), 477 (sh, 230), 491 (250), 506 (290), 531 (sh, 290), 546 (370), 597 (sh, 190), 614 (270). IR (KBr): 2107 (C≡C). ^{1}H-NMR (360 MHz): 0.997 (*s*, 84 H). ^{13}C-NMR (90.6 MHz): 11.06; 18.51; 87.80; 94.05; 99.67; 106.8; 124.4. DEI-MS (20 eV): 868 (M^+). X-Ray: *Fig. 2*.

The yellow fraction was evaporated: **5** (0.104 g, 12%). Greasy solid. M.p. 215° (dec.). UV/VIS (pentane): 323 (13500), 356 (sh, 17000), 367 (sh, 25000), 375 (sh, 35700), 383 (52700), 405 (115200), 425 (sh, 15200), 438 (33600), 453 (34000). IR (KBr): 2122 (C≡C). ^{1}H-NMR (360 MHz): 1.170 (*s*, 126 H). ^{13}C-NMR (90.6 MHz): 11.31; 18.69; 83.81; 85.09; 102.3; 107.4; 118.0. DEI-MS (20 eV): 1303 (M^+).

1,2,7,8,13,14-Hexaethynyl-3,4,5,5,9,10,11,12,15,16,17,18-dodecadehydro[18]annulene (**6**). To a soln. of **4** (0.1 g, 0.13 mmol) in MeOH/THF 5:1 (50 ml) was added 0.02M $Na_2B_4O_7$ (4.02 mg) in H_2O (1 ml). After 50 min, TLC (SiO_2, hexane/CH_2Cl_2 5:1) indicated complete conversion. The soln. was poured into $CDCl_3$ and extracted with H_2O (8×), concentrated, filtered through a short plug (SiO_2, $CDCl_3$), and concentrated to 10 ml. A sample of this yellow soln. was used for NMR spectroscopy. At −20° in the dark for 1 h, the soln. decomposed by turning to dark-brown. IR (hexane): 3299 (≡C–H), 2111 (C≡C). ^{1}H-NMR (500 MHz): 3.502 (*s*, 6 H). ^{13}C-NMR (125.8 MHz): 78.75; 84.07; 84.47; 90.39; 118.7.

*(Z)-1,4-Bis[(*tert*-butyl)dimethylsilyloxy]-2,3-dichlorobut-2-ene* (**21**). To a soln. of **20** [21] (3.14 g, 20 mmol) in DMF (20 ml) was added (*t*-Bu)Me_2SiCl (7.5 g, 50 mmol) and 1*H*-imidazole (4.0 g, 58 mmol). The mixture was stirred for 5 d, then poured into Et_2O, and extracted with ice-cold H_2O (4×). The org. layer was dried ($MgSO_4$) and evaporated to yield a yellow oil which was flushed through a plug (SiO_2, CH_2Cl_2): **21** (6.8 g, 88%). Colorless oil. ^{1}H-NMR (500 MHz): 0.12 (*s*, 12 H); 0.92 (*s*, 18 H); 4.45 (*s*, 4 H). ^{13}C-NMR (125.8 MHz); −5.32; 18.30; 25.75; 63.43; 133.2. EI-MS (20 eV): 327/329 ([M − *t*-Bu]$^+$). HR-MS: 327.0786 ([M − *t*-Bu]$^+$, $C_{12}H_{25}Cl_2O_2Si_2^+$; calc. 327.0770).

*(Z)-1,6-Bis(trimethylsilyl)-3,4-bis{[(*tert*-butyl)dimethylsilyloxy]methyl}hex-3-ene-1,5-diyne* (**22**). To a carefully degassed soln. of **21** (3 g, 7.8 mmol) in benzene (400 ml) were added sequentially $BuNH_2$ (3 g, 41 mmol), [$PdCl_2(PPh_3)_2$] (0.1 g, 0.14 mmol), CuI (0.1 g, 0.5 mmol), and Me_3Si–C≡CH (2.3 g, 23.4 mmol), and the mixture was stirred at r.t. und a positive pressure of N_2 for 18 h. The soln. was filtered through a plug (SiO_2, hexane then CH_2Cl_2). The CH_2Cl_2 fraction was evaporated and the resulting oil filtered through a 2nd plug (SiO_2, hexane, then hexane/CH_2Cl_2 1:1): **22** (2.9 g, 73%). Colorless oil. IR (neat): 2133 (C≡C). ^{1}H-NMR (500 MHz): 0.096 (*s*, 18 H); 0.21 (*s*, 12 H); 0.91 (*s*, 18 H); 4.29 (*s*, 4 H). ^{13}C-NMR (125.8 MHz): −5.25; −0.19; 18.32; 25.85; 61.42; 101.5; 104.3; 130.8. EI-MS: (20 eV): 508 (2, M^+), 451 (50, [M − *t*-Bu]$^+$), 73 (100, Me_3Si^+). HR-MS: 508.2917 (M^+, $C_{26}H_{52}O_2Si_4^+$; calc. 508.3044).

*(Z)-3,4-Bis{[(*tert*-butyl)dimethylsilyloxy]methyl}hex-3-ene-1,5-diyne* (**23**). To a stirred soln. of **22** (2 g, 4 mmol) in MeOH (50 ml) was added K_2CO_3 (50 mg, 0.36 mmol). After 7 h, TLC (hexane/Et_2O 10:1) indicated complete deprotection. The mixture was poured into hexane and extracted with H_2O (4×). Drying ($MgSO_4$) and evaporation yielded **23** (1.4 g, 98%). Yellow oil which solidified at −15°. IR (neat): 3300 (≡C–H), 2133 (C≡C). ^{1}H-NMR (500 MHz): 0.10 (*s*, 12 H); 0.91 (*s*, 18 H); 3.35 (*s*, 2 H); 4.34 (*s*, 4 H). ^{13}C-NMR (125.8 MHz): −5.29; 18.31; 25.83; 61.48; 82.81; 83.74; 130.8. EI-MS: (20 eV): 349 (1, $[M - Me]^+$), 307 (15, $[M - t\text{-Bu}]^+$), 73 (100, Me_3Si^+). HR-MS: 364.2233 (M^+, $C_{20}H_{36}O_2Si_2^+$; calc. 364.2254).

*1,2,7,8-Tetrakis{[(*tert*-butyl)dimethylsilyloxy]methyl}-3,4,5,6,9,10,11,12-octadehydro[12]annulene* (**18**) *and 1,2,7,8,13,14-hexakis{[(*tert*-butyl)dimethylsilyloxy]methyl}-3,4,5,6,9,10,11,12,15,16,17,18-dodecadehydro[18]-annulene* (**19**). To a stirred soln. of **23** (1 g, 2.7 mmol) in acetone (400 ml) open to the air was added *Hay* catalyst (1 ml, *ca.* 0.2 mmol; prepared as described for the synthesis of **1** and **4**). After 12 h at r.t., the solvent was evaporated to 20 ml and then the mixture poured into hexane and extracted with H_2O (2×). The org. layer was filtered through a plug (SiO_2), first with hexane to yield a light-pink fraction, then with hexane/Et_2O 5:1 to give a bright-yellow fraction. The pink fraction was evaporated, and recrystallization gave **18** (685 mg, 69%). Deep-orange crystals. M.p. 157° (dec.). UV/VIS (hexane): 247 (24500), 269 (sh, 5300), 287 (6200), 305 (6300), 344 (sh, 350), 403 (130), 448 (200), 480 (180), 504 (160), 560 (70). IR (KBr): 2177, 2111 (C≡C). ^{1}H-NMR (200 MHz): 0.01 (*s*, 24 H); 0.83 (*s*, 36 H); 3.61 (*s*, 8 H). ^{13}C-NMR (50 MHz): −5.3; 18.60; 25.89; 59.56; 86.54; 96.13; 139.4. EI-MS (20 eV): 724 (M^+), 667 ($[M - t\text{-Bu}]^+$). Anal. calc. for $C_{40}H_{68}O_4Si_4$ (725.32): C 66.24, H 9.45; found: C 66.49, H 9.18.

The yellow fraction was evaporated, and recrystallization afforded **19** (80 mg, 8%). Yellow powder. M.p. 220° (dec.). UV/VIS (hexane): 234 (24600), 308 (sh, 25900), 330 (sh, 54100), 345 (89800), 398 (62900). IR (KBr): 2178, 2111 (C≡C). ^{1}H-NMR (500 MHz): 0.165 (*s*, 36 H); 0.957 (*s*, 54 H); 4.83 (*s*, 12 H). ^{13}C-NMR (50 MHz): −5.16; 18.34; 25.85; 62.14; 82.63; 84.77; 132.3. MALDI-TOF-MS: 857 ($[M - 4t\text{-Bu}]^-$). Anal. calc. for $C_{60}H_{102}O_6Si_6 \cdot CH_2Cl_2$ (1172.92): C 62.47, H 8.94; found: C 62.26, H 8.39.

Attempts to Prepare the Expanded Radialenes **7**–**9**. a) *By* Eglinton-Glaser *Coupling*. To a soln. of **24** [21] (366 mg, 0.839 mmol) in pyridine (100 ml) was added anh. $Cu(OAc)_2$ (3.0 g, 16.57 mmol). After stirring for 24 h at r.t., the mixture was poured into pentane/H_2O and washed several times with 30% aq. $CuSO_4$ soln., H_2O, and sat. aq. NaCl soln. Upon concentration and filtration through a plug (SiO_2, hexane), the resulting yellow oil rapidly turned dark.

b) *By* Cadiot-Chodkievicz *Hetero-coupling*. To a soln. of **25** [21] (125 mg, 0.210 mmol) and **24** [21] (108 mg, 0.247 mmol) in DMF/benzene 1:1 (50 ml) was added $NH_2OH \cdot HCl$ (4 mg, 0.057 mmol), CuCl (5.6 mg, 0.057 mmol), and $BuNH_2$ (2 drops). After stirring for 24 h, the mixture was poured into Et_2O/H_2O and washed with H_2O, followed by sat. aq. NaCl soln. TLC analysis showed complete decomposition.

5,10,15,20-Tetrakis{3-(triisopropylsilyl)-1-[(triisopropylsilyl)ethynyl]prop-2-ynylidene}cycloicosa-1,3,6,8-11,13,16,18-octayne (**7**) *and 5,10,15,20,25,30-Hexakis{3-(triisopropylsilyl)-1-[(triisopropylsilyl)ethynyl]prop-2-ynylidene}cyclotriaconta-1,3,6,8,11,13,16,18,21,23,26,28-dodecayne* (**9**). To a soln. of anh. $Cu(OAc)_2$ (35.2 mg, 0.194 mmol) in freshly distilled pyridine/benzene 3:1 (8 ml) was added over 4 h a soln. of **26** [8] (17.9 mg, 0.021 mmol) in benzene (2 ml). After stirring at r.t. for 20 h, the mixture was poured into 30% aq. $CuSO_4$ soln., washed with 30% aq. $CuSO_4$ soln. (3×), H_2O (1×), and sat. aq. NaCl soln. (1×). After drying ($MgSO_4$) and evaporation, the formed oil was passed through a plug (flash SiO_2, hexane). The bright-yellow product mixture was further purified by chromatography (reversed-phase SiO_2, CH_2Cl_2/MeCN 2:1 then 3:1) to give four fractions.

Fr. 1 (R_f 0.31, reversed-phase SiO_2, CH_2Cl_2/MeCN 2:1) gave **7** (2.6 mg, 15%). Stable yellow solid. M.p. > 260°. UV/VIS (hexane): 212 (sh, 90000), 227 (sh, 51800), 247 (sh, 25500), 292 (31200), 308 (32700), 357 (sh, 28700), 385 (sh, 55300), 418 (115300), 438 (72700), 451 (77200). FT-IR (CCl_4): 2125 (C≡C). ^{1}H-NMR (400 MHz): 1.09 (*s*, 168 H). ^{13}C-NMR (100.6 MHz): 11.2; 18.6; 84.1; 85.7; 103.4; 106.6; 115.0; 118.4. LD-TOF-MS: 1739 (M^-). Anal. calc. for $C_{112}H_{168}Si_8$ (1739.27): C 77.35, H 9.74; found: C 77.22, H 9.95.

Fr. 2 (R_f 0.19, reversed-phase SiO_2, CH_2Cl_2/MeCN 2:1) gave **9** (3.4 mg, 20%). Stable yellow solid. M.p. > 260°. UV/VIS (hexane): 215 (sh, 120600), 225 (122000), 246 (106400), 258 (93100), 275 (81200), 307 (78700), 349 (sh, 116800), 373 (186900), 392 (183300), 408 (sh, 119000), 422 (sh, 96800), 446 (77700). FT-IR (neat): 2124 (C≡C). ^{1}H-NMR (300 MHz): 1.10 (*s*, 252 H). ^{13}C-NMR (100.6 MHz): 11.2; 18.6; 82.3; 83.2; 103.0; 106.1; 115.1; 121.8. LD-TOF-MS: 2608 (M^-). Anal. calc. for $C_{168}H_{252}Si_{12}$ (2608.91): C 77.35, H 9.74; found: C 77.52, H 9.72.

Fr. 3 (R_f 0.31, reversed-phase SiO_2, CH_2Cl_2/MeCN 3:1) presumably is a higher expanded radialene formed by cyclization of 4 equiv. of **26**: 3.0 mg (17%). Stable yellow solid. FT-IR (neat): 2127 (C≡C). ^{1}H-NMR (300 MHz): 1.10 (*s*). LD-TOF-MS: 3475 (M^-, $C_{224}H_{336}Si_{16}$; calc. 3474.26).

Fr. 4 (R_f 0.21, reversed-phase SiO_2, CH_2Cl_2/MeCN 3:1) gave a mixture of the oligomer of *Fr. 3* and two larger compounds **A** (major product) and **B**, presumably formed by cyclization of 5 and 6 equiv. of **26**, resp. Stable yellow

solid. FT-IR (neat): 2125 (C≡C). ^{1}H-NMR (300 MHz): 1.10 (*s*). LD-TOF-MS: 3475 (33, M^-, $C_{224}H_{336}Si_{16}^-$; calc. 3474.26), 4344 (100, **A**, M^-, $C_{280}H_{420}Si_{20}^-$; calc. 4342.82), 5215 (33, **B**, M^-, $C_{336}H_{504}Si_{24}^-$; calc. 5211.39).

5,10,15,20,25-Pentakis{3-(triisopropylsilyl)-1-[(triisopropylsilyl)ethynyl]prop-2-ynylidene}cyclopentacosa-1,3,6,8,11,13,16,18,21,23-decayne (**8**). To **27** [8] (50 mg, 0.033 mmol) was added MeOH/THF 1:1 (40 ml) and K_2CO_3 (91 mg, 0.66 mmol). After stirring for 1 h at r.t., the mixture was poured into pentane/H_2O 1:1 and washed with H_2O and sat. aq. NaCl soln. Drying and evaporation gave **28** as an unstable oil for immediate use in the following reaction. To a soln. of anh. $Cu(OAc)_2$ (100 mg, 0.55 mmol) in freshly distilled pyridine/benzene 3:1 (40 ml) was added a soln. of **26** [8] (29 mg, 0.033 mmol) and freshly prepared **28** (*ca.* 0.033 mmol) in benzene (10 ml). After stirring for 20 h at r.t., the mixture was worked up as described for **7** and **9**. The bright-yellow soln. obtained after the first plug filtration was chromatographed (reversed-phase SiO_2, CH_2Cl_2/MeCN 2:1, then 3:1): **8** (9.2 mg, 15%). Stable yellow solid. M.p. > 260°. R_f 0.25 (reversed-phase SiO_2, CH_2Cl_2/MeCN 2:1). UV/VIS (hexane): 216 (sh, 110500), 225 (103500), 245 (sh, 58700), 309 (61600), 351 (sh, 70200), 376 (108700), 393 (sh, 116800), 407 (143300), 428 (106200), 441 (107800). FT-IR (neat): 2121 (C≡C). ^{1}H-NMR (500 MHz): 1.10 (*s*, 210 H). ^{13}C-NMR (125.8 MHz): 11.2; 18.6; 83.2; 83.5; 103.3; 106.4; 114.8; 120.7. LD-TOF-MS: 2174 (M^-). Anal. calc. for $C_{140}H_{210}Si_{10}$ (2174.09): C 77.35, H 9.74; found: C 77.44, H 9.79.

REFERENCES

[1] M. J. Bucknum, R. Hoffmann, *J. Am. Chem. Soc.* **1994**, *116*, 11456, and ref. cit. therein.

[2] F. Diederich, *Nature (London)* **1994**, *369*, 199.

[3] Z. Wu, S. Lee, J. S. Moore, *J. Am. Chem. Soc.* **1992**, *114*, 8730; J. Zhang, J. S. Moore, *ibid.* **1994**, *116*, 2655; Z. Xu, M. Kahr, K. L. Walker, C. L. Wilkins, J. S. Moore, *ibid.* **1994**, *116*, 4537; J. Zhang, D. J. Pesak, J. L. Ludwick, J. S. Moore, *ibid.* **1994**, *116*, 4227.

[4] R. H. Baughman, D. S. Galvao, *Nature (London)* **1993**, *365*, 735.

[5] U. H. F. Bunz, *Angew. Chem.* **1994**, *106*, 1127; *ibid. Int. Ed.* **1994**, *33*, 1073.

[6] A. de Meijere, S. Kozhushkov, C. Puls, T. Haumann, R. Boese, M. J. Cooney, L. T. Scott, *Angew. Chem.* **1994**, *106*, 934, *ibid. Int. Ed.* **1994**, *33*, 869.

[7] J. A. Anthony, C. Boudon, F. Diederich, J.-P. Gisselbrecht, V. Gramlich, M. Gross, M. Hobi, P. Seiler, *Angew. Chem.* **1994**, *106*, 794; *ibid. Int. Ed.* **1994**, *33*, 763.

[8] A. M. Boldi, J. Anthony, V. Gramlich, C. B. Knobler, C. Boudon, J.-P. Gisselbrecht, M. Gross, F. Diederich, *Helv. Chim. Acta* **1995**, *78*, 779.

[9] F. Sondheimer, *Acc. Chem. Res.* **1972**, *5*, 81.

[10] H. A. Staab, J. Ipaktschi, A. Nissen, *Chem. Ber.* **1971**, *104*, 1182.

[11] M. Nakagawa, *Angew. Chem.* **1979**, *91*, 215; *ibid. Int. Ed.* **1979**, *18*, 202.

[12] A. G. Myers, N. S. Finney, *J. Am. Chem. Soc.* **1992**, *114*, 10986; Y. Kuwatani, N. Watanabe, I. Ueda, *Tetrahedron Lett.* **1955**, *36*, 119.

[13] J. Anthony, C. B. Knobler, F. Diederich, *Angew. Chem.* **1993**, *105*, 437; *ibid. Int. Ed.* **1993**, *32*, 406.

[14] F. Diederich, Y. Rubin, *Angew. Chem.* **1992**, *104*, 1123; *ibid. Int. Ed.* **1992**, *31*, 1101.

[15] H. Hopf, G. Maas, *Angew. Chem.* **1992**, *104*, 953; *ibid. Int. Ed.* **1992**, *31*, 931.

[16] E. Heilbronner, *Theor. Chim. Acta (Berlin)* **1966**, *4*, 64.

[17] T. Lange, V. Gramlich, W. Amrein, F. Diederich, M. Gross, C. Boudon, J.-P. Gisselbrecht, *Angew. Chem.* **1995**, *107*, 898; *ibid. Int. Ed.* **1995**, *34*, 805.

[18] A. M. Boldi, F. Diederich, *Angew. Chem.* **1994**, *106*, 482; *ibid. Int. Ed.* **1994**, *33*, 468.

[19] R. L. Lagow, J. J. Kampa, H.-C. Wei, S. L. Battle, J. W. Genge, D. A. Laude, C. J. Harper, R. Bau, R. C. Stevens, J. F. Haw, E. Munson, *Science (Washington D.C.)* **1995**, *267*, 362.

[20] A. S. Hay, *J. Org. Chem.* **1962**, *27*, 3320.

[21] J. Anthony, A. M. Boldi, Y. Rubin, M. Hobi, V. Gramlich, C. B. Knobler, P. Seiler, F. Diederich, *Helv. Chim. Acta* **1995**, *78*, 13.

[22] a) O. M. Behr, G. Eglinton, A. R. Galbraith, R. A. Raphael, *J. Chem. Soc.* **1960**, 3614; b) W. K. Grant, J. C. Speakman, *Proc. Chem. Soc. London* **1959**, 231.

[23] Q. Zhou, P. J. Carroll, T. M. Swager, *J. Org. Chem.* **1994**, *59*, 1294.

[24] Y. Li, Y. Rubin, F. Diederich, K. N. Houk, *J. Am. Chem. Soc.* **1990**, *112*, 1618.

[25] D. R. M. Walton, F. Waugh, *J. Organomet. Chem.* **1972**, *37*, 45.

[26] R. Boese, J. R. Green, J. Mittendorf, D. L. Mohler, K. P. C. Vollhardt, *Angew. Chem.* **1992**, *104*, 1643; *ibid. Int. Ed.* **1992**, *31*, 1643.

[27] P. Garratt, P. Vollhardt, 'Aromatizität', Thieme Verlag, Stuttgart, 1973.
[28] H. Ajie, M.M. Alvarez, S.J. Anz, R.D. Beck, F. Diederich, K. Fostiropoulos, D.R. Huffman, W. Krätschmer, Y. Rubin, K.E. Schriver, D. Sensharma, R.L. Whetten, *J. Phys. Chem.* **1990**, *94*, 8630; J. Catalan, J.L. Saiz, J.L. Laynez, N. Jagerovic, J. Elguero, *Angew. Chem.* **1995**, *107*, 86; *ibid. Int. Ed.* **1995**, *34*, 86.
[29] F. Diederich, Y. Rubin, O.L. Chapman, N.S. Goroff, *Helv. Chim. Acta* **1994**, *77*, 1441; Y. Rubin, F. Diederich, *J. Am. Chem. Soc.* **1989**, *111*, 6870; Y. Rubin, M. Kahr, C.B. Knobler, F. Diederich, C.L. Wilkins, *ibid.* **1991**, *113*, 495.
[30] W.H. Okamura, F. Sondheimer, *J. Am. Chem. Soc.* **1967**, *89*, 5991; H.P. Figeys, M. Gelbcke, *Tetrahedron Lett.* **1970**, 5139.
[31] a) K.G. Untch, D.C. Wysocki, *J. Am. Chem. Soc.* **1966**, *88*, 2608; b) F. Sondheimer, R. Wolovsky, P.J. Garratt, I.C. Calder, *ibid.* **1966**, *88*, 2610.
[32] G.M. Pilling, F. Sondheimer, *J. Am. Chem. Soc.* **1971**, *93*, 1970.
[33] H.A. Staab, R. Bader, *Chem. Ber.* **1970**, *103*, 1157.
[34] C. Boudon, J.P. Gisselbrecht, M. Gross, J. Anthony, A.M. Boldi, R. Faust, T. Lange, D. Philp, J.-D. van Loon, F. Diederich, *J. Electroanal. Chem.*, in press.
[35] R.D. Allendoerfer, P.H. Riger, *J. Am. Chem. Soc.* **1965**, *87*, 2336; J.F.M. Oth, H. Baumann, J.M. Gilles, G. Schröder, *ibid.* **1972**, *94*, 3498; J.F.M. Oth. E.P. Woo, F. Sondheimer, *ibid.* **1973**, *95*, 7337.
[36] K. Sonogashira, in 'Comprehensive Organic Synthesis', Ed. B.M. Trost, Pergamon, New York, 1991, Vol. 3, pp. 551–561; D. O'Krongly, S.R. Denmeade, M.Y. Chiang, R. Breslow, *J. Am. Chem. Soc.* **1985**, *107*, 5544.
[37] a) W. Chodkievicz, *Ann. Chim. (Paris)* **1957**, *2*, 819; b) F. Bohlmann, P. Herbst, H. Gleinig, *Chem. Ber.* **1961**, *94*, 948; c) J.A. Miller, G. Zweifel, *Synthesis* **1983**, 128; d) U. Niedballa, in 'Houben-Weyl, Methoden der Organischen Chemie', Eds. E. Müller and O. Bayer, Thieme, Stuttgart, 1977, Vol. V/2a, pp. 913–962.
[38] F. Diederich, R. Ettl, Y. Rubin, R.L. Whetten, R. Beck, M. Alvarez, S. Anz, D. Sensharma, F. Wudl, K.C. Khemani, A. Koch, *Science (Washington D.C.)* **1991**, *252*, 548; F. Diederich, U. Jonas, V. Gramlich, A. Hermann, H. Ringsdorf, C. Thilgen, *Helv. Chim. Acta* **1993**, *76*, 2445.
[39] R.J. Cotter, *Anal. Chem.* **1992**, *64*, 1027A; F. Hillenkamp, M. Karas, R.C. Beavis, B.T. Chait, *ibid.* **1991**, *63*, 1193A.
[40] H.N.C. Wong, F. Sondheimer, *Tetrahedron* **1981**, *37* (Suppl. No. 1), 99.
[41] M. Schreiber, J. Anthony, F. Diederich, M.E. Spahr, R. Nesper, M. Hubrich, F. Bommeli, L. Degiorgi, P. Wachter, P. Kaatz, C. Bosshard, P. Günter, M. Colussi, U.W. Suter, C. Boudon, J.-P. Gisselbrecht, M. Gross, *Adv. Mater.* **1994**, *6*, 786.
[42] Q. Xie, F. Arias, L. Echegoyen, *J. Am. Chem. Soc.* **1993**, *115*, 9818; A. Hirsch, 'The Chemistry of the Fullerenes', Thieme, Stuttgart, 1994, Chapt. 2, pp. 37–54.